Investigation of Activation Cross-Sections of Alpha-Induced Nuclear Reactions on Natural Silver

Muhammad Shahid[a], Kwangsoo Kim[a], Haladhara Naik[a,b], Muhammad Zaman[a], Sinchul Kang[a], Changgi Huh[a], Guinyun Kim[a*]

[a] *Department of Physics, Kyungpook National University, Daegu 702-701, Republic of Korea*
[b] *Radiochemistry Division, Bhabha Atomic Research Centre, Mumbai 400085, India*
Corresponding author: gnkim@knu.ac.kr

1. Introduction

We investigated the production cross sections and excitation functions of ^{108m,108g,109g,110m,110g,111g}In, ^{109g,111m}Cd and ^{105g,106m,110m,111g}Ag from alpha-induced reactions on ^{nat}Ag from their respective threshold to 44.8 MeV. The purpose was to study the production route of some radioisotopes applicable in medicine and industry. The measured results were compared with literature data and theoretical values. The ^{nat}Ag(α,x) reaction has already been studied for different energy ranges. However, the literature data needed new data set to increase the reliability of the reported results. The current experimental work will be helpful to make the literature data more reliable and to modify the theoretical models.

2. Materials and Methods

A high-purity (99.95 %) Silver foil (10-µm thickness) with a size of 1.0 cm ×1.0 cm was used as a target material. Natural copper foils (>99.9 % purity, 10-µm thickness) with a size of 1.0 cm ×1.0 cm were used as a flux monitor and an energy degrader. The sequence of the Silver and Copper foils in a stack was designed on the basis of threshold values for the products from ^{nat}Ag(α,x) and ^{nat}Cu(α,x) reactions. The stack composed of 13 sets of Ag-Cu followed by four Ag foils. The purpose of multiple monitor foils (Eα = 43.6 - 14.1 MeV) was to decrease unknown systematic errors in activity measurement. The estimated average energy loss in each foil for Cu and Ag foils was in the range of 0.46 - 1.03 MeV and 0.47 – 2.41 MeV respectively.
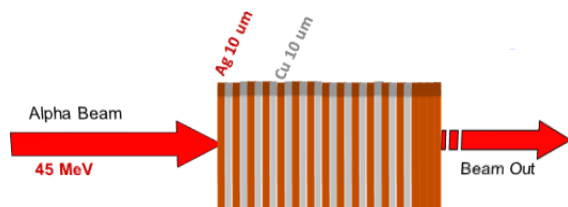
Fig. 2.1. The arrangement of target (^{nat}Ag) and monitor (^{nat}Cu) foils in the stack designed for the activation with alpha beam of 45MeV

The stack was irradiated by 44.8 MeV alpha beam collimated to 10 mm in diameter and about 200 nA beam current for 30 min in the external beam line of the MC-50 cyclotron at Korean Institute of Radiological and Medical Sciences (KIRAMS), Korea [1]. The beam energy, current and experimental conditions were kept constant during the irradiation. The irradiation geometry was designed so that the foils in the sample get the maximum beam.
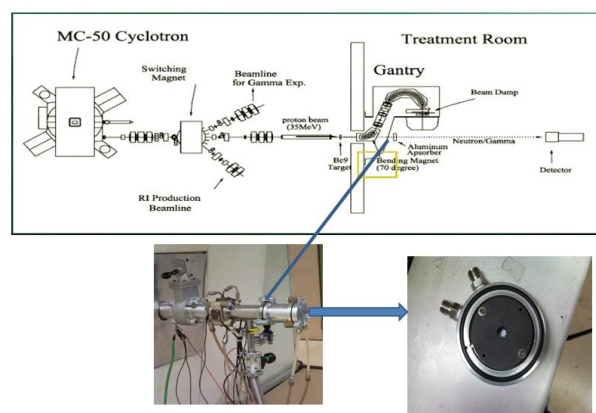
Fig. 2.2. The layout (up) and external beam line (down left) of MC-50 cyclotron at Korean Institute of Radiological and Medical Sciences (KIRAMS), Korea.

3. Data Acquisition and Analysis

After irradiation and an appropriate cooling time, the irradiated foils were removed and measured by using an n-type coaxial HPGe gamma-ray spectrometer couple to a PC-based 4096 channel analyzer with the associated electronics to determine the photo-peak area of the gamma ray spectrum by using the Gamma vision 5.0 (EG&G Ortec) program. The energy resolution of the detector was 1.9 keV full width at half maximum (FWHM) at the 1332.5 keV gamma-ray photo-peak of ^{60}Co. The photo-peak efficiency curve of the γ-ray spectrometer was determined at the different distances using the standard gamma source ^{152}Eu having gamma-rays in the energies range of 121.8 – 1408.0 keV.
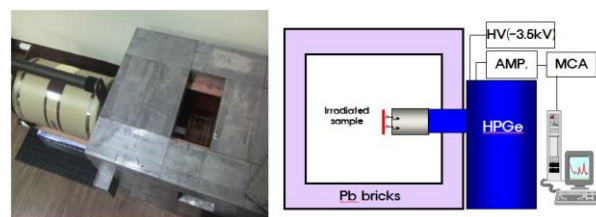
Fig. 3.1. The lead shielded high purity germanium (HPGe)

detector (left) and layout with associated electronics (right)

The activity measurements of the irradiated samples were started after 1.37 hours from the end of the bombardment (EOB). The measurements of the activated targets and monitor foils were repeated several times within 3 years to follow the decay of the radionuclides and thereby to identify the possible interfering nuclides. The alpha beam flux and energy was estimated by using three monitor reactions such as $^{nat}Cu(\alpha,x)^{65}Zn$, $^{nat}Cu(\alpha,x)^{66}Ga$ and $^{nat}Cu(\alpha,x)^{67}Ga$ recommended by IAEA [2].

4. Results and Discussion

The cross-sections were determined using the well-known activation formula [3].

$$\sigma(E_i) = \frac{\lambda\, C(E_i)}{\varepsilon(E_i)\, I_\gamma\, \rho\, t\, \varphi \left(1 - e^{-\lambda t_m}\right) e^{-\lambda t_C} \left(1 - e^{-\lambda t_{irr}}\right)}$$

where λ is the decay constant (s^{-1}), $C(E_i)$ is the net counts under the photo-peak area at the i-th sample, $\varepsilon(E_i)$ is the detection efficiency of the HPGe-detector, I_γ is the γ-ray intensity, ρ is the atomic density, t is the target foil thickness (cm), φ is the proton beam intensity (p s^{-1}), t_c is the cooling time (s), t_m is the counting time (s), and t_{irr} is the irradiation time (s). The interferences were subtracted using the following relation:

$$C(E_{\gamma 1}) = C(E_{\gamma 2}) \times \frac{\varepsilon(E_{\gamma 1}) \times I_{\gamma 1}}{\varepsilon(E_{\gamma 2}) \times I_{\gamma 2}}$$

Where $C(E_\gamma)$ is decay corrected counts. The decay data relevant for the cross-sections determination was taken from the ENSDF evaluation obtained from the NuDat-2.6 library [4]. The Q-values and threshold energies calculated on the basis of the atomic mass evaluation by Wang et al. and the Q-tool system [5]. Intensity and independent characteristic gamma-lines were used to quantify the radionuclides. In some cases, two or more characteristic gamma-rays were used to check the obtained results. From the measured cross section values, the integral yields for ^{108m,108g,109g,110m,110g,111g}In, ^{109g,111m}Cd and ^{105g,106m,110m,111g}Ag was also determined as a function of the alpha energy.

The estimated uncertainty of a representing point in the alpha energy for Silver foils was in the range of ±0.47 – 2.41 MeV. The combined uncertainty in each cross-section was estimated by considering the following uncertainties; statistical uncertainty of the gamma-ray counting (0.30~24.25 %), uncertainties in the alpha beam intensity (~5.30 %), in the efficiency calibration of the detector (4~5 %), due to the sample thickness (1~2 %), and in gamma intensity (~1 %). The overall uncertainties of the measured cross-sections were in the range of 6.8~25.4 %.

The experimental results measured in this work were compared with the literature data and also theoretical values obtained from TENDL-2013 library [6] based on the computer code TALYS-1.6 [7]. The integral yields for thick target of the investigated radioisotopes were calculated from the excitation function and the electronic stopping power.

The experimentally determined Independent and cumulative cross-sections for production of radioisotopes of Indium, Cadmium and Silver by irradiation of Silver with alpha particles are measured. The estimated uncertainties in energy and cross-section values are also presented. The data were plotted as a function of α-particle energy and the excitation curves thus obtained were compared with experimental data and also with theoretical data in the TENDL-2013 library as shown in Figs. 4.1–4.12. The integral yields for thick targets are also determined using the measured production cross-sections and the stopping power of ^{nat}Ag over the energy region from a threshold to the initial alpha energy by taking into account that the total energy is absorbed in the target and they are shown in Figs. 4.13–4.15.

4.1 $^{nat}Ag(\alpha,x)^{108}In$ Reaction

The measured cross-sections for the formation of ^{108m}In are plotted in Fig. 4.1 while for ^{108g}In are given in Fig. 4.2.
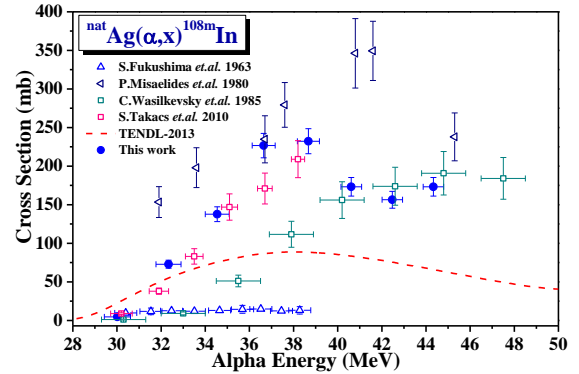
Fig. 4.1 Excitation function of the $^{nat}Ag(\alpha,x)^{108m}In$ reaction
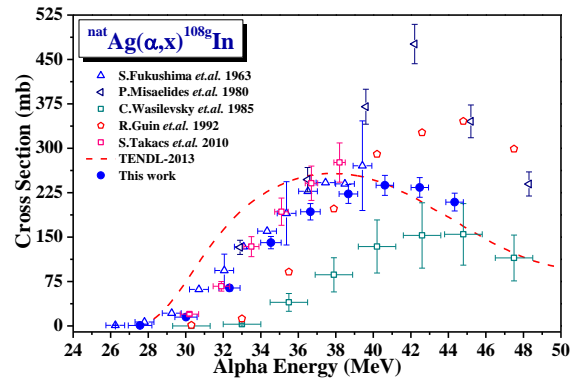
Fig. 4.2 Excitation function of the $^{nat}Ag(\alpha,x)^{108g}In$ reaction

4.2. ^{nat}Ag(α,x)^{109}In Reaction

The values of the production cross-sections are graphically presented in Fig. 4.3 with the literature data and theoretical model calculations.
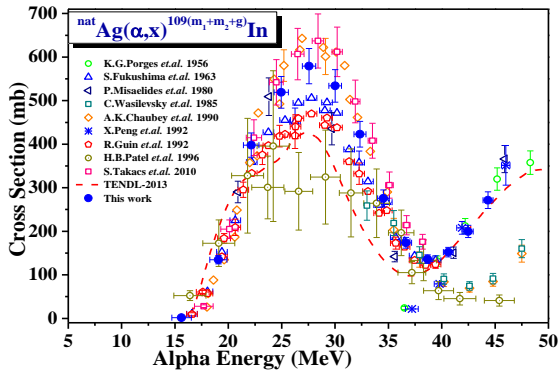
Fig. 4.3 Excitation function of the ^{nat}Ag(α,x)$^{109(m1+m2+g)}$In reaction

4.3. ^{nat}Ag(α,x)^{110}In Reaction

The values of the ^{110m}In measurements are graphically plotted in Fig. 4.4 while the results for ^{110g}In are plotted in Fig. 4.5 with literature data and theoretical model calculations.
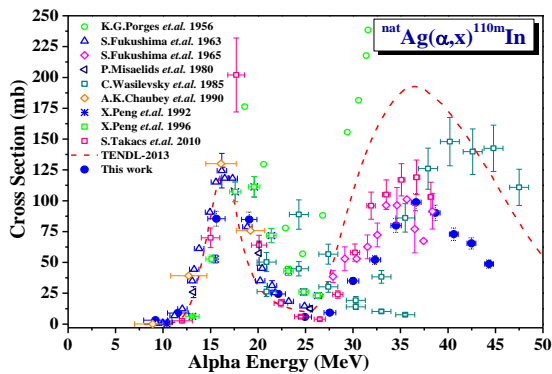
Fig. 4.4 Excitation function of the ^{nat}Ag(α,x)^{110m}In reaction
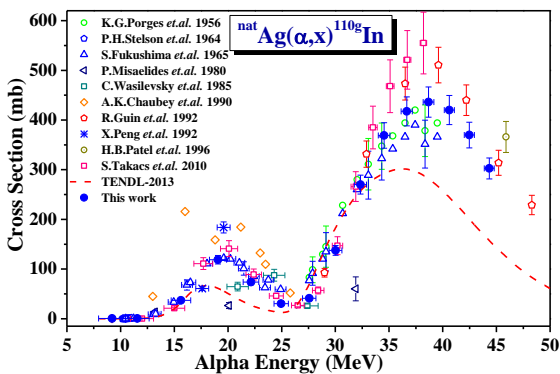
Fig. 4.5 Excitation function of the ^{nat}Ag(α,x)^{110g}In reaction

.

4.4. ^{nat}Ag(α,x)^{111}In Reaction

Supposing the production of ^{111m}In, the measured excitation functions are cumulative of metastable and ground state. The results are plotted in Fig. 4.6.
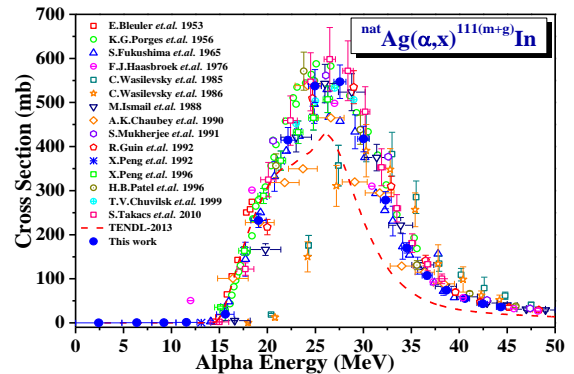
Fig. 4.6 Excitation function of the ^{nat}Ag(α,x)$^{111(m+g)}$In reaction

4.5. ^{nat}Ag(α,x)^{109}Cd Reaction

The measured production cross-sections of ^{109}Cd are graphically presented in Fig. 4.7 together with the literature data and theoretical model calculations.
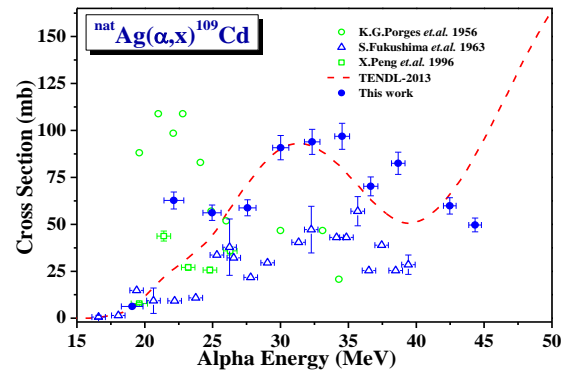
Fig. 4.7 Excitation function of the ^{nat}Ag(α,x)^{109}Cd reaction

4.6. ^{nat}Ag(α,x)^{111m}Cd Reactions

The measured production cross-sections of ^{111m}Cd are graphically shown in Fig. 4.8 in comparison with the available experimental data. Currently theoretical model calculations are not available for ^{111m}Cd therefore; the calculations for total (ground + level 3) are plotted
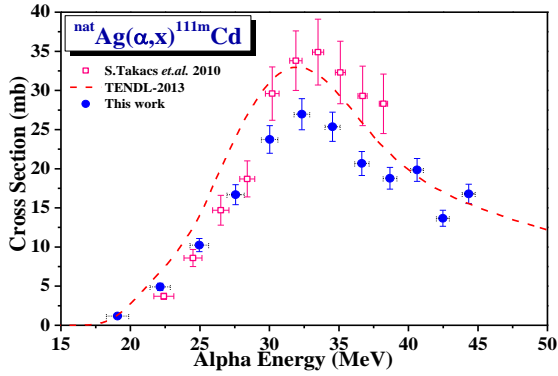
Fig. 4.8 Excitation function of the ^{nat}Ag(α,x)^{111m}Cd reaction

4.7. ^{nat}Ag(α,x)^{105}Ag Reaction

The production of meta stable state was not identified in this work because off line spectrometric technique was applied. However, supposing its production the cumulative production cross-sections are graphically presented in Fig. 4.9 with literature data and theoretical measurements.
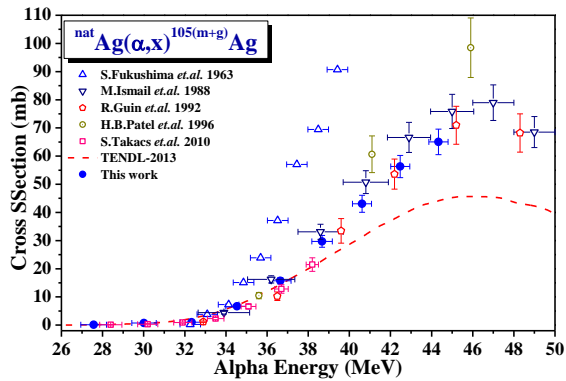
Fig. 4.9 Excitation function of the ^{nat}Ag(α,x)$^{105(m+g)}$Ag reaction

4.8. ^{nat}Ag(α,x)^{106m}Ag Reaction

The production cross-section of ^{nat}Ag(α,x)^{106m}Ag reaction are graphically plotted in Fig. 4.10 compared with the literature data and the theoretical model calculations.
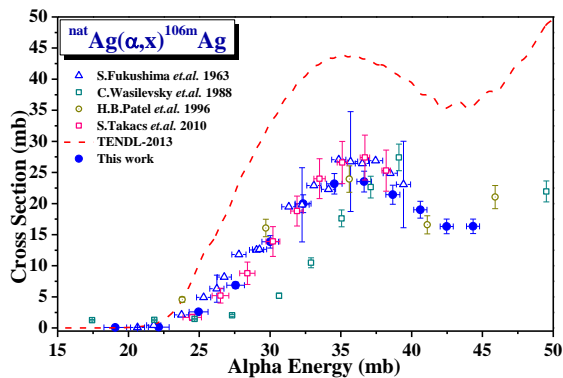
Fig. 4.10 Excitation function of the ^{nat}Ag(α,x)^{106m}Ag reaction

4.9. ^{nat}Ag(α,x)^{110m}Ag Reactions

The production cross-sections of ^{nat}Ag(α,x)^{110m}Ag reactions are graphically presented in Fig. 4.11 in comparison with the literature data and theoretical model calculations. Currently TALYS-1.6 does not calculate cross section values for ^{110m}Ag therefore, the plotted values are for Level-2 of ^{110}Ag.
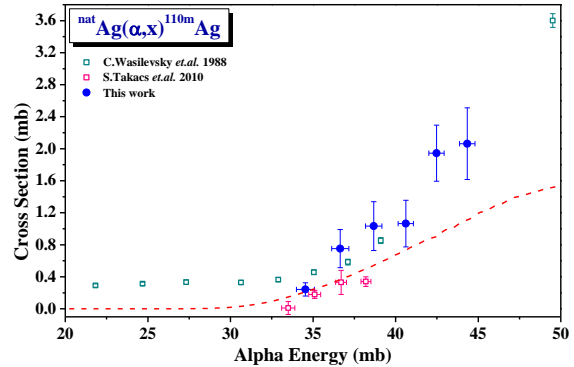
Fig. 4.11. Excitation function of the ^{nat}Ag(α,x)^{110m}Ag reaction

4.10. ^{nat}Ag(α,x)^{111}Ag Reaction

The meta stable state ^{111m}Ag was not identified because offline spectrometry system was applied however, its production was assumed. The values of the cumulative production cross-section are graphically presented in Fig. 4.12 with the literature data and theoretical model calculations.
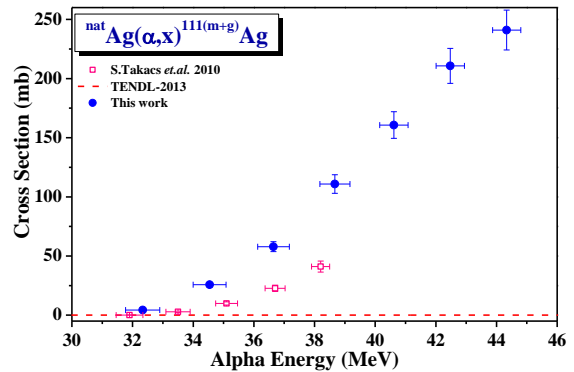
Fig. 4.12 Excitation function of the ^{nat}Ag(α,x)$^{111(m+g)}$Ag reaction

4.11. Integral Yields for Thick Target

The physical integral yield for thick target of the produced radioisotope was determined by:

$$Y = I_\alpha \cdot N_d \cdot \int_{E_{th}}^{E_{in}} \frac{\sigma(E)}{(dE/dx)_E} dE \times \lambda$$
,

where I_α is the number of incident α-particles per a constant charge (1A x 1h), $(dE/dx)_E$ is the stopping power of each target sample (MeV/cm), dE is the energy difference between two successive target (MeV) The integral yield was finally obtained in unit of Bq/μA.h that can be converted to MBq/μA·h. The Figs. 4.13-4.15 show the integral yield for In, Cd and Ag reaction products respectively in comparison with literature data.
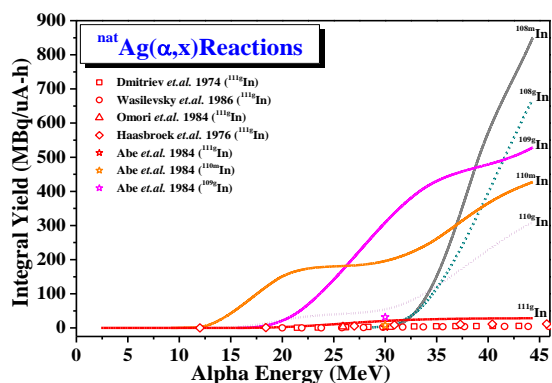
Fig. 4.13 Integral yield of In reaction products in ^{nat}Ag(α,x) reaction.
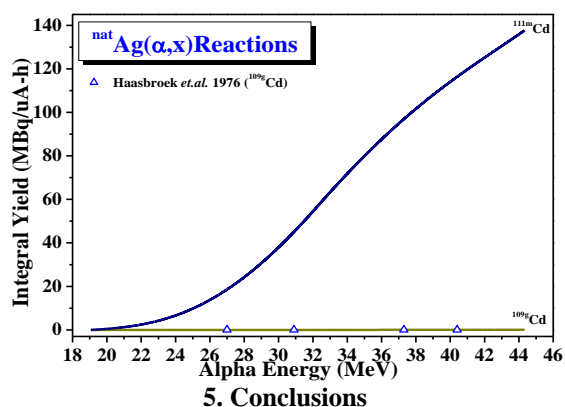
Fig. 4.14 Integral yield of Cd reaction products in ^{nat}Ag(α,x) reaction.
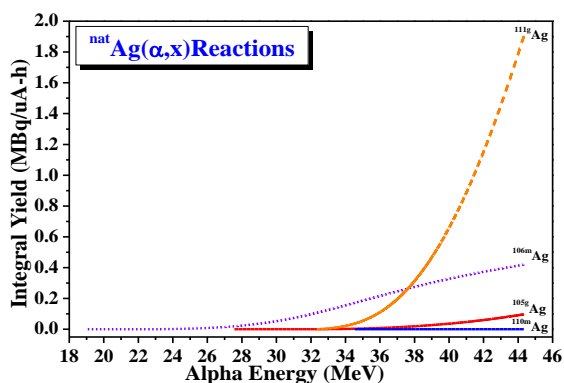
Fig. 4.14 Integral yield of Ag reaction products in ^{nat}Ag(α,x) reaction.

5. Conclusions

We have measured the production cross-sections of the ^{108m,108g,109g,110m,110g,111g}In, ^{109g,111m}Cd and ^{105g,106m,110m,111g}Ag radionuclides from ^{nat}Ag(α,x) nuclear reactions in the energy region from their threshold energy to the 44.8 alpha energy by using a stacked-foil activation technique with overall uncertainties in the range of 6.8 – 25.4 %. The investigated ^{87,88}Y and ^{88,89}Zr radionuclides have significance due to their potential applications in diagnosis and therapy. The ^{nat}Ag(α,x) reaction has already been studied for different energy ranges. However, the literature data needed new data set to increase the reliability of the reported results. The current experimental work is helpful to make the literature data more reliable and to modify the theoretical models.

REFERENCES

[1] C. Lee, J. C. Kim, J. H. Ha, J. H. Park, S. H. Park, Y. D. Kim, J. Y. Huh, J. H. Lee, C. S. Lee, H. Y. Lee, S. A. Shin, J. S. Chai, Y. S. Kim, Molecular Ion Beam Extraction from the KCCH MC-50 Cyclotron J. Korean Phys. Soc. Vol. 35, p. 105 199 9.
[2] Charged particle cross-section database for medical radioisotope production: diagnostic radioisotopes and monitor reactions IAEA-TECDOC-1211, 2001.
[3] G. Gilmore, J. D. Hemingway, Practical Gamma-Ray Spectrometry, Chapter 1, John Wiley and Sons, England, pp. 17. 1995.
[4] A. A. Sonzogni, NuDat 2.0: Nuclear Structure and Decay Data on the Internet, International Conference on Nuclear Data for Science and Technology, CP769 .
[5] Qtool: Calculation of Reaction Q-values and thresholds, Los Alamos National Laboratory, T-2 Nuclear Information Service. Available from: <http://www.nndc.bnl.gov/qcalc/ >.
[6] A. J. Koning, D. Rochman, S. C van der Marck, J. Kopecky, J. Ch. Sublet, S. Pomp, H. Sjostrand, R. Forrest, E. Bauge, H. Henriksson, O. Cabellos, S. Goriely, J. Leppanen, H. Leeb, A. Plompen, R. Mills, TENDL-2013: TALYS-based evaluated nuclear data library, Nuclear Research and Consultancy Group (NRG), Petten. Netherlands, 2013
[7] A. J. Koning, S. Hilaire, M. C. Duijvestijn, TALYS-1.0, in O. Bersillon, F. Gunsing, E. Bauge, R. Jacqmin,S. Leray (Eds.), Proceedings of the International Conference on Nuclear Data for Science and Technology, EDP Science, Nice, France, pp. 211-214 2007.